

The plastic behaviour of silicon subjected to micro-indentation

L. ZHANG, M. MAHDI

Centre for Advanced Materials Technology, Department of Mechanical and Mechatronic Engineering, The University of Sydney, NSW 2006, Australia

Micro-indentation is widely used in evaluating the mechanical properties of ceramics. It is also an important measure in the study of machinability of brittle materials. Because of the complexity of interaction in the vicinity of the contact zone between the indenter and work material, an analytical or experimental method is unable to predict the detailed evolution process of deformation. With the aid of the finite element method, this paper analyses the behaviour of a silicon subjected to micro-indentation by a spherical indenter. The development of stress fields was thoroughly simulated. A constitutive relationship was confirmed based on a comparison with experimental observations. This study offers essential information for the indentation of ceramics and a deeper understanding of material removal mechanisms in machining brittle materials.

1. Introduction

Micro-indentation is widely used to provide information for evaluating a variety of mechanical properties of materials such as wear, machinability, erosion, fracture and so forth. It has become particularly important in recent years as hard brittle materials such as advanced ceramics have become widely used in industry. Theoretical and semi-empirical analyses of general indentation problems have received extensive attention. Hill *et al.* [1] have produced a detailed analysis of a flat punch indentation under plane strain conditions. Shield [2] has discussed the case of axisymmetric indentation. Johnson [3] has performed a comprehensive semi-empirical study and suggested a formula for correlating experimental observations on hardness. Recently, based on the spherical cavity solution proposed by Hill [4], Chiang *et al.* [5] investigated the response of solids to elastic/plastic spherical indentation. Their analysis permitted relations to be established between material properties (hardness, yield strength and elastic modulus) and the dimensions of the indentation and plastic zone. All of these studies were performed on ductile materials.

In the indentation of brittle materials, cracking is a major problem. Perrott [6] attempted to generate information on the stress field and the information contained therein about the indentation fracture. However, the assumption used in this study is not consistent with real conditions. Very few solutions under real stress–strain relations are reported due to the complexity of deformation in the vicinity of the contact zone. An adequate numerical analysis is therefore required. An interesting discussion by Bhattacharya and Nix [7] on cone indentation highlighted

the use of the finite element method in dealing with indentation processes.

In machining processes such as cutting, grinding and polishing, any changes in the mechanism of material removal is always of great concern in brittle materials [8,9]. The use of plastic deformation before the onset of cracking is critical to a machining process that aims at obtaining damage-free machined surfaces [9] (e.g., ductile-regime cutting and grinding). Micro-indentation has been found to be a useful tool to elucidate the change in material removal mechanism between brittle and ductile modes. Some approximate formulae for calculating the threshold of transition were established based on indentation [10,11]. However, the lack of precise knowledge about the development of deformation in the indentation zone limits the usefulness of these formulae. Moreover, an invalid assumption that the relationship between the hardness and yield stress for ductile materials remains true for brittle materials is still in common use.

The purpose of this paper is to investigate the micro-indentation of brittle materials. The development of deformation zones is studied through a simulation with the aid of finite element techniques. The von Mises yield function is used to predict plastic behaviour which is confirmed by experimental results available. The evolution of stress fields is simulated and analysed for the onset of plasticity and cracking. A comparison of frictionless and frictional indentations gives rise to a detailed examination of the effect of interface friction. This research offers valuable information for a more practical application of indentation mechanics to the evaluation of mechanical properties of hard and brittle materials.

2. Modelling with finite element method

Because of the symmetry of deformation, a micro-indentation problem with a spherical indenter of radius R was modelled as an axisymmetric contact problem between two bodies of revolution. This is shown in Fig. 1, where axisymmetric conditions have been taken into account, P is the indentation load, a is the radius of projection of the contact zone, and u and v are displacements in the r and z directions respectively. The dimensions of the workpiece subjected to indentation were considered to be infinite as compared to those of the contact zone. However, for the sake of convenience of the finite element calculation, a finite control volume bounded by $0 \leq r \leq r_{cv}$ and $0 \leq z \leq z_{cv}$ must be used, where r_{cv} and z_{cv} are positive constants such that the vertical displacement, $v(r, z_{cv})$, and the radial and shear stresses, $\sigma_r(r_{cv}, z)$ and $\tau_{r\theta}(r_{cv}, z)$, are approximately zero. ($r_{cv} = z_{cv} = 3.5R$ were used in this study.)

The indentation process was considered to be quasi-static and the indenter as being perfectly rigid. A high stress concentration was expected in the vicinity of the contact zone, thus a very fine mesh was used in this zone which became coarser further away, see Fig. 2. An axisymmetric 9-node element was used, which was found to be the most effective when computational efficiency and accuracy were considered. A calculation was considered to have converged when a further refinement of the mesh brought about a negligible difference between two subsequent solutions. With the above specified control volume, a total of 432 elements led to reliable results. All the computations were carried out using the ADINA code in a Sun SPARC Station 1 computer. The profile of a half of the hemispherical rigid indenter was simulated by 192 quadratic segment curves (385 nodes in total).

In a loading process, a series of downward increments in the rigid body displacement was imposed on the indenter to induce the indentation into the workmaterial. In an unloading process, the reverse process operated i.e., the indenter was moved gradually upwards. In both the loading and unloading processes, the step size of the displacement increment was determined by the convergence

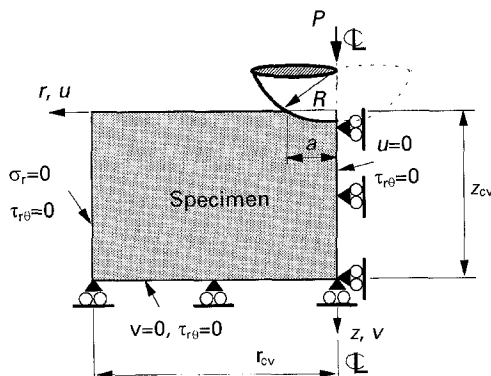


Figure 1 The indentation model.

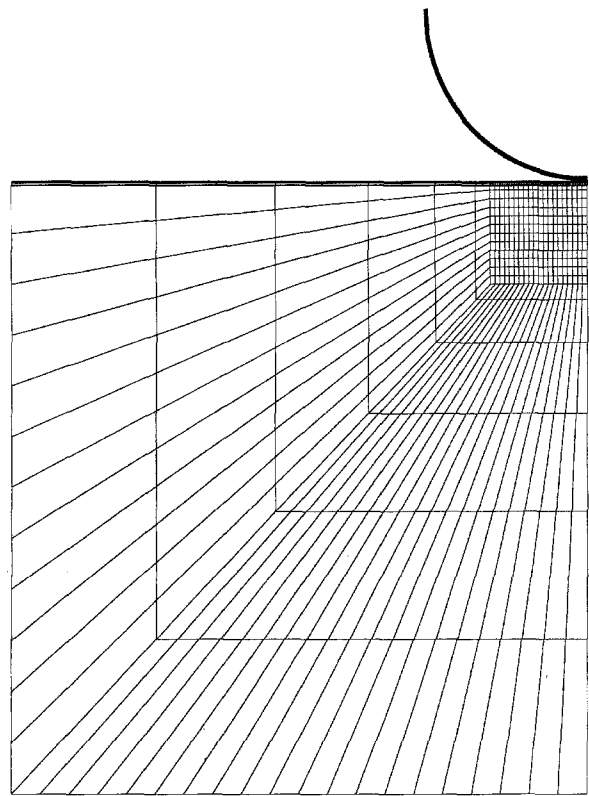


Figure 2 The finite element mesh.

criterion that a further refinement of the increment would only have a negligible effect on the overall result.

3. Results and discussion

Silicon is selected as the workmaterial in this study (the corresponding experimental work is reported in reference [12]). Its Young's modulus, E , is 153 GPa and its Poisson's ratio, ν , 0.22. The material is assumed to be isotropic and the radius of the hemispherical indenter, R , is 8.5 μm .

3.1. Constitutive model

A constitutive relationship is not available for studying the irreversible deformation of silicon prior to fracture (this is true for the whole class of ceramic materials, to the authors' knowledge), which correlates the tensors of stress rate and strain rate defined by continuum mechanics. The main reason for this is that yielding of a silicon can only occur at a high temperature or a high hydrostatic stress level. It is therefore impossible to obtain a yield stress for silicon using a uniaxial tensile test at ambient temperature, which is the universal method for defining yielding of ductile materials.

The von Mises yield criterion, usually applied to metallic materials, has been applied to brittle materials such as concrete [13]. The von Mises criterion depends only on the second stress invariant and does not include any effect of hydrostatic stress. However, one of the most important problems in using this criterion for brittle materials such as silicon is how to

determine the yield stress defined by the uniaxial test and the associated flow rule corresponding to the subsequent yielding. To overcome this difficulty, we introduce an *equivalent yield stress* (EYS) to replace the usual yield stress in the von Mises function. This EYS is a comprehensive physical quantity that integrates the irreversible deformation induced by either the plasticity and densification and therefore differs from both the classical concept of uniaxial yield stress for ductile materials and that of pure plastic yielding under a high hydrostatic stress for brittle materials. An analytical expression of the equivalent yield stress needs a further rigorous theoretical investigation. For the given material studied in this paper, however, the specific value of the EYS can be determined by the comparison of a theoretical calculation with an indentation test.

The obtained EYS of silicon subjected to indentation was 5.4 GPa. The indentation force-displacement curve shown in Fig. 3 is in very good agreement with the experimental results [12]. Therefore, the von Mises function simulates closely the response of the silicon to indentation. The onset of irreversible deformation ($P = 0.014$ N) is much lower than the macroscopic bifurcation point Q ($P = 0.075$ N) on the experimental curve. Furthermore, theoretical analysis does not show any bifurcation, although plastic yielding was taken into account. Therefore, in addition to plastic yielding, the bifurcation on the experimental curve reflects some other effects such as micro-cracking.

3.2. Evolution of stress field

The evolution of the principal stress field during loading and unloading is clearly demonstrated in Fig. 4. Stresses are highly compressive and the hydrostatic stress is extremely large. At the beginning of loading, the tensile stress field is small and close to the boundary of the indentation interface, thus a propagation of existing surface cracks, if any, may be expected. At point B of the loading curve in Fig. 3, a considerable tensile stress field is developed beneath the indentation interface. This is the main source of initial cracking during loading. When unloading progresses, the tensile stress field develops further towards the indentation surface, and at the same time, the directions of

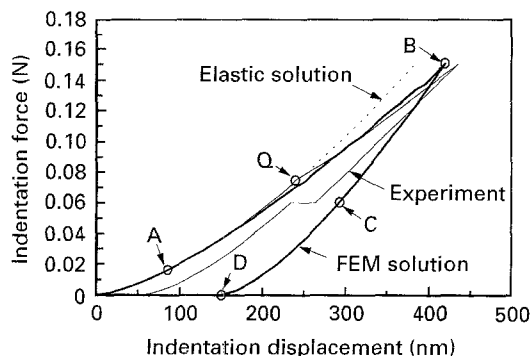


Figure 3 The indentation force-displacement curve.

both the compressive and tensile stresses change. The magnitude of the maximum tensile stress, σ_m , grows quickly as well. At point C of the unloading curve, σ_m becomes remarkable and may cause a further cracking. This may be the reason for the large step change observed experimentally [12]. When the material is completely unloaded (point D in Fig. 3), the direction of the tensile stress becomes perpendicular to the contact surface and that of compressive stress is almost parallel to the surface. Such a stress distribution can easily cause delamination of the work-material parallel to the indentation surface.

It is of interest to note that there are usually no grooves on the ground surfaces of extremely brittle materials, see for example, the ground SiC surfaces shown in Fig. 5. Nevertheless, clear marks of delamination are often observed. According to the experimental detection by Imanaka [14] in grinding glass components, a considerable number of chips burst out from the glass surface after the cutting edge had passed over. By recalling the distribution of residual stresses in Fig. 4, such a chipping process can be considered as the result of delamination induced by the residual stress field after complete unloading. Similarly, in a wear process of two mating surfaces, delamination is also a major wear mechanism. The above discussion indicates that wear delamination may also be caused by the penetration of hard asperities on the mating surfaces.

3.3. Development of plastic zone

It is important to note that the maximum effective stress appears first at a point below the indentation interface. Hence, initial yielding does not occur on the interface. The distribution of the accumulated effective plastic strain illustrated by Fig. 6 shows that the boundary profile of the final plastic zone is close to a spheroidal surface though it is not so at its initial stage of development (see Fig. 7). The strain distribution in the plastic zone is not uniform. The maximum plastic strain zone is near the contact interface, as indicated by the very narrow black band in Fig. 6. Furthermore, the profile of the plastic zone is greatly dependent on the level of the indentation load. When the indentation load is relatively large, the profile can be assumed to be spheroidal in a mechanics analysis. However, an error will be introduced if this assumption is applied to the case with a small load.

3.4. Relationship between the indentation stress and strain

The relationship between the indentation stress, $P/\pi a^2$, and the indentation strain, a/R , is shown in Fig. 8. A bifurcation from the linear Hertzian solution occurs at point Q*. This bifurcation point corresponds to $P = 0.014$ N which is the exact indentation load for initiating irreversible deformation according to von Mises criterion. Therefore, the indentation stress at Q* serves as an indication for determining the equivalent yield stress of a brittle material when

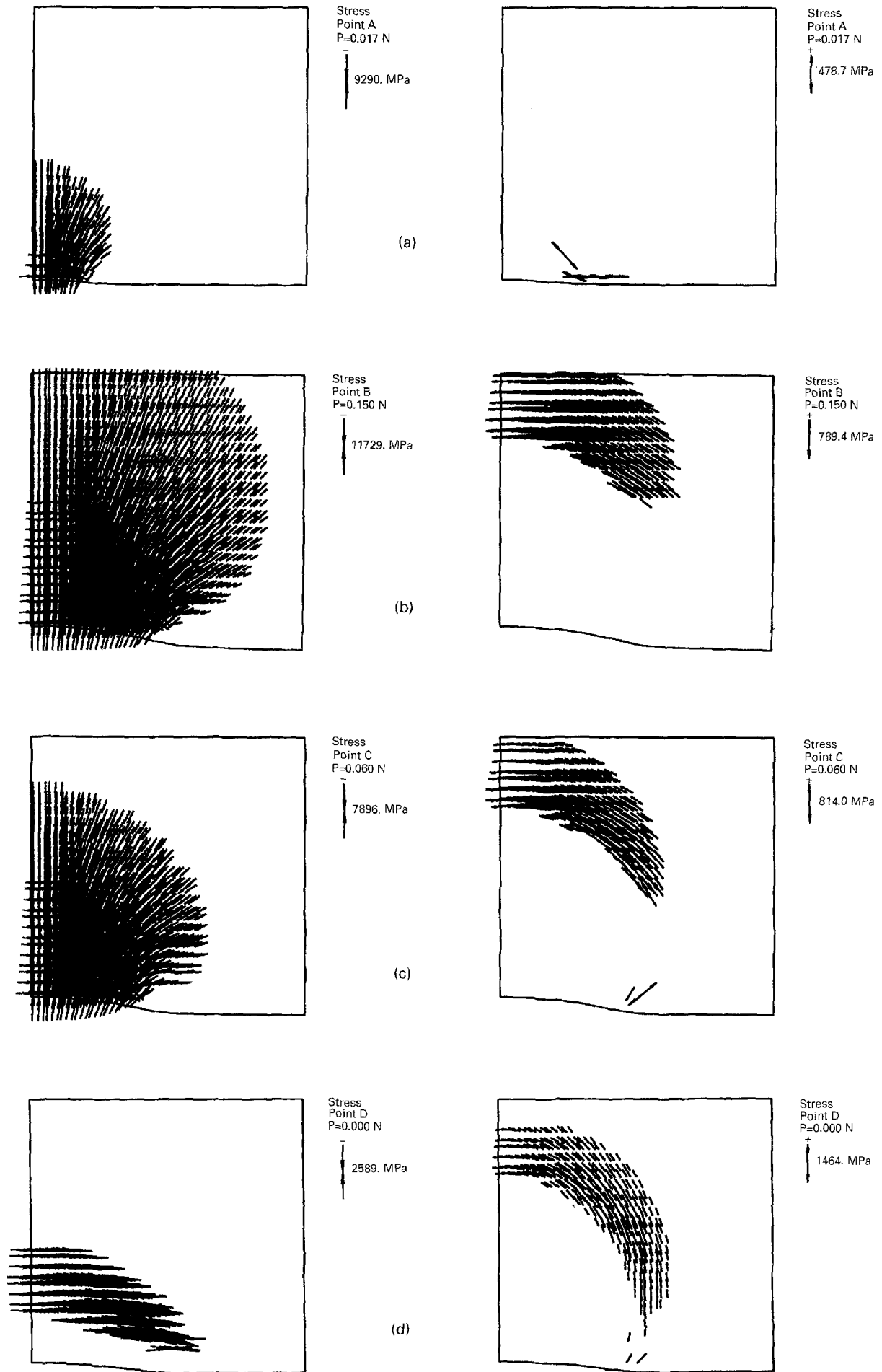


Figure 4 Principal stresses at different indentation load levels. (a) $P = 0.017$ N (loading) (b) $P = 0.15$ N (loading) (c) $P = 0.06$ N (unloading) (d) $P = 0$ (completely unloaded).

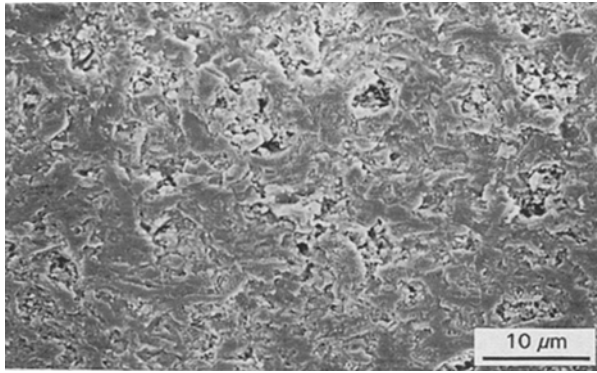


Figure 5 The ground surface of SiC (grinding condition: table speed: 1 mm per s, depth of wheel cut: 1 mm, diamond grinding wheel: MDY170Q5SV5, coolant: NET909 (PH: 8.9) × 30 water).

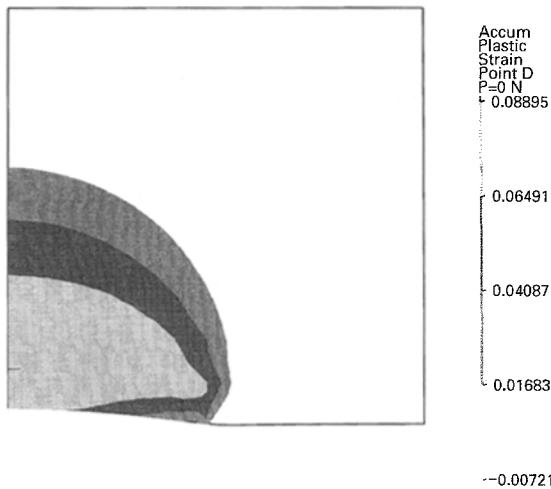


Figure 6 The distribution of effective plastic strain after complete unloading.

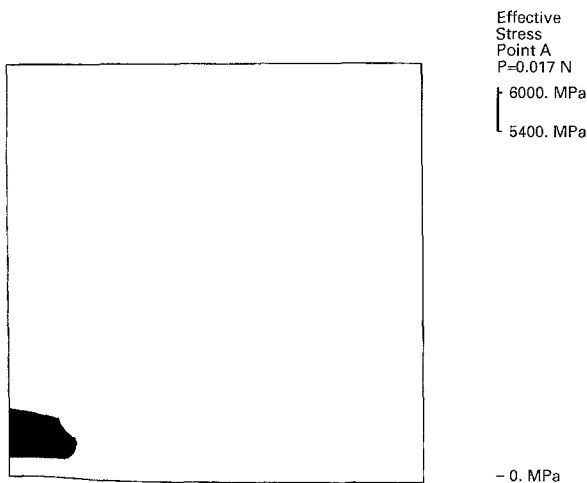


Figure 7 The plastic zone in an early loading stage ($P = 0.017$ N).

a micro-indentation test is used. However, as mentioned earlier, the bifurcation point Q in Fig. 3 does not imply the onset of irreversible deformation.

3.5. Effect of interface friction

The above results are obtained based on an assumption that the indentation is frictionless. This is not true

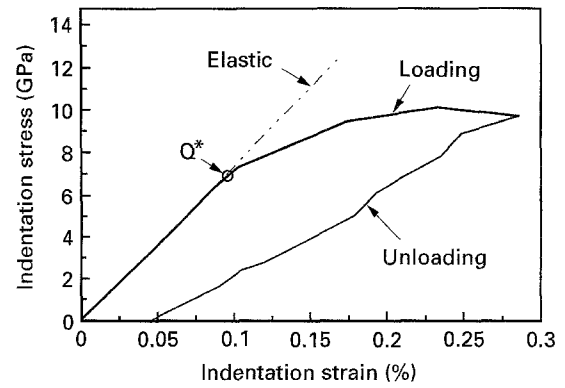


Figure 8 The indentation stress–strain relationship.

in practice. Further calculations with different friction coefficients show that the effect of interface friction is negligible in terms of the indentation load–displacement relationship and the stress and strain distributions with a certain distance away from the contact surface. However, the friction has a large effect on the stresses in the neighbourhood of the indentation interface, particularly near the contact boundary. The interface friction restrains the free sliding of the contact surfaces and hence creates additional tensile stresses on the surface of the workmaterial and increases the possibility of surface cracking during loading.

4. Conclusions

The conclusions that can be drawn from this work are;

1. The von Mises function can accurately predict the irreversible deformation of silicon subjected to a micro-indentation;
2. The bifurcation point, Q^* , on the indentation stress–strain curve indicates accurately the onset of irreversible deformation;
3. The direction of the tensile residual stress field is almost perpendicular to the indentation surface whilst that of the compressive is parallel to the surface. Such a distribution of residual stresses may easily cause fracture delamination;
4. The friction between the surfaces of the indenter and workmaterial has a large effect on the stresses in the vicinity of the indentation interface. It creates additional tensile stresses on the workpiece surface and increases the possibility of surface cracking during loading.

Acknowledgement

The support of the Australian Research Council Large Grant Scheme is appreciated.

References

1. R. HILL, E. H. LEE and S. J. TUPPER, *Trans ASME, J. Appl. Mech.* **18** (1951) 46.
2. R. T. SHIELD, *Proc. R. Soc. A* **233** (1955) 267.
3. K. L. JOHNSON, *J. Mech. Phys. Solids* **11** (1970) 115.
4. R. HILL, “*The Mathematical Theory of Plasticity*”, (Clarendon, Oxford, 1950).

5. S. S. CHIANG, D. B. MARSHALL and A. G. EVANS, *J. Appl. Phys.* **53** (1982) 298.
6. C. M. PERROTT, *Wear* **45** (1977) 293.
7. A. K. BHATTACHARYA and W. D. NIX, *Int. J. Solids Structures* **27** (1991) 1047.
8. L. C. ZHANG, T. SUTO, H. NOGUCHI and T. WAIDA, *Manufacturing Review* **5** (1992) 261.
9. L. C. ZHANG, in Proceedings of the International Ceramics Conference, edited by C. C. Sorrell and A. J. Ruys, Australian Ceramic Society, Sydney (1994) 1377.
10. J. T. HAGAN, *J. Mater. Sci.* **14** (1979) 2975.
11. S. S. CHIANG, D. B. MARSHALL and A. G. EVANS, *J. Appl. Phys.* **53** (1982) 312.
12. E. R. WEPPELMANN, J. S. FIELD and M. V. SWAIN, in *Ceramics: Adding the Value*, edited by M. J. Bannister, CSIRO Publication, Melbourne (1992) 944.
13. M. LABBANE, N. K. SAHA and E. C. TING, *Int. J. Solids Structures* **30** (1993) 1269.
14. O. IMANAKA, in Proceedings of the 2nd International Conference on Machine Tools Engineers, Japan Society of Mechanical Engineers, Kobe, Japan (1986) 88.

*Received 25th May 1995
and accepted 18th March 1996*